

SUITABILITY OF A PROFILE WITH TUBERCLES FOR AXIAL PUMPS - INVESTIGATION USING FLOW SIMULATION

Mareen DERDA¹, Ferdinand NEUMANN², Paul Uwe THAMSEN³

¹ Corresponding Author. Department of Fluid System Dynamics, Institute of Fluid Dynamics and Technical Acoustics, Technische Universität Berlin. Straße des 17. Juni 135, 10623 Berlin, Germany. Tel.: +49 30 314 27832, E-mail: mareen.derda@tu-berlin.de

² E-mail: ferdinand.neumann@campus.tu-berlin.de

³ Department of Fluid System Dynamics, Institute of Fluid Dynamics and Technical Acoustics, Technische Universität Berlin., E-mail: paul-uwe.thamsen@tu-berlin.de

ABSTRACT

Even if wind tunnel tests and simulations have confirmed that tubercles can influence the behaviour of a profile, research in the field of axial pumps has so far been lacking. However, previous studies cannot be transferred to the application in axial pumps, since the requirements for the profile geometry as well as the Reynolds number range differ. The present study aims to address this research gap by performing a CFD simulation with a profile common for axial pumps, the Goe11K, testing four different tubercle configurations. At the same time, this simulation is a preliminary study for experimental tests.

The results show that certain tubercle configurations improve the behaviour of the profile in the post-stall area, i.e. increase the lift of the profile at large angles of attack (α). In general, the curve of the profiles with tubercles runs more evenly, without the drastic drop in lift. This improved property comes at the expense of lower maximum lift and increased drag at lower α . With regard to the use in axial pumps, it can be concluded that there are advantages particularly in the partial load range. That could ultimately enlarge the operation range of an axial pump.

Keywords: axial pumps, CFD, tubercles

NOMENCLATURE

A	$[m]$	tubercle amplitude
c	$[m]$	chord length
c_D	$[-]$	coefficient of drag
c_L	$[-]$	coefficient of lift
d_A	$[mm]$	outer pump diameter
k	$[J/kg]$	turbulent kinetic energy
L	$[m]$	characteristic length
n	$[1/min]$	rotational speed
Δp	$[kg/m \cdot s^2]$	pressure difference to ambience
Re	$[-]$	Reynolds number

u	$[m/s]$	freestream velocity
w	$[m]$	tubercle wavelength
y^+	$[-]$	dimensionless wall distance
α	$[^\circ]$	angle of attack
ν	$[m^2/s]$	kinematic viscosity
ρ	$[kg/m^3]$	density
ω	$[1/s]$	specific dissipation rate

1. INTRODUCTION

Previous research by Fish et al. [1] and many others have already shown that sinusoidal wing leading edges, modeled after the leading edge of humpback whale fins and called tubercles, can strongly influence flow behaviour. The earlier study has shown that the tubercles change the stall and post-stall behaviour of a wing resulting in a smoother flow separation and an increased post-stall lift [1].

However, the known research on the application of tubercles in pumps is limited and non-existent for axial pumps. Due to the different profile selection, results from existing studies cannot be relied on when designing axial pump blades with tubercles. Therefore, this study aims to address that research gap by using CFD-methods on an infinite vane with a Goe11K, a profile commonly used in axial pumps, within a Reynolds number region of $Re = 1.5 \cdot 10^6$ and an α range from 0° to 24° . Since axial pumps represent a wide area of application and therefore an important area of research, this is a first step towards the investigation of the suitability of tubercled profiles for axial pumps. Based on this, experimental investigations are to be carried out.

2. STATE OF RESEARCH

2.1. Basic Mechanism of Tubercles

In the previous research literature, four mechanisms of action of tubercles are mainly distinguished. The first effect was mentioned by van Nierop et al. [2]. It was claimed that the pressure

distribution on the wing in flow direction, which is different behind tubercle tips and valleys, influences the separation behaviour. Due to a higher pressure gradient behind the tubercle valleys the flow separates there first while still staying attached behind the tips. This contributes to the smoother separation characteristics of a tubercled wing.

The second effect was mentioned by Miklosovic et al. [3]. The resulting vortices behind the tubercle valleys are thought to increase the momentum exchange between boundary layer and freestream near the trailing edge of the wing, resulting the flow staying attached in these regions at higher α . This working mechanism is comparable to the one of “vortex generators”.

A third working mechanism was mentioned by Pedro et al. [4]. The vortices, which appear behind tubercle valleys, work as a barrier against spanwise flow on a wing like wing fences. Therefore, on finite wings tubercles reduce the expansion of separation zones along the wingspan resulting in an increased lift at high α , where parts of a finite wing are already stalled. It must be noted that this effect only shows in experiments and simulations with finite wings with changing profile contour along the span. As a result, those phenomena will not occur in the presented simulation approach, where the wing profile does not change along the span. Therefore, no spanwise pressure gradient and no changeable separation behaviour along wingspan can be expected, which tubercles could potentially help reducing.

The fourth effect was described by Custodio [5]. The author argues that the vortices accelerate the flow on the wing, resulting in lower pressure and lift often called “vortex lift”.

2.2. Influence of Tubercles on the Behaviour of a Profile

The before mentioned study by Miklosovic et al. [3] has shown, how tubercles can improve the flow around a wing. In their research a finite wing with a NACA 0012 profile, with a maximum thickness of 12% at 30% chord length, was tested in a wind tunnel at a Reynolds number range from $Re = 1.35 \cdot 10^5$ up to $Re = 5 \cdot 10^5$. The Reynolds number is defined as the ratio of inertial forces to viscous forces and can be calculated with Eq. (1).

$$Re = \frac{u \cdot L}{\nu} \quad (1)$$

The wing with tubercles showed an increased maximum lift by 6% and a decreased drag up to 32% at high α . In addition, the stall characteristic of the wing was smoother on the wing with tubercles than on the one without. At low α the tubercles did not show a change in lift and drag when compared with the non-modified wing.

A study by Cai et al. [6] tested the influence of tubercles on an infinite wing with a NACA 63₄-021 profile at Reynolds number $Re = 2 \cdot 10^5$ using CFD-methods. The results in this research show a different influence of the tubercles on wing performance. At high α , where the flow on the unmodified wing is still attached, the tubercled wing has an increased drag and reduced lift. The tubercles show an improved flow behaviour only in the region of separated flow, where drag is like the unmodified wing while lift is increased.

Those two studies highlight, that the influence of tubercles on the wing characteristics is not the same for all applications, but rather depend on parameters like the selected airfoil, Reynolds number and test setup.

The influence of tubercles on flow characteristics also depends on the geometry of the tubercles defined by the amplitude A and the wavelength w . Both parameters are annotated in Figure 1 for better understanding.

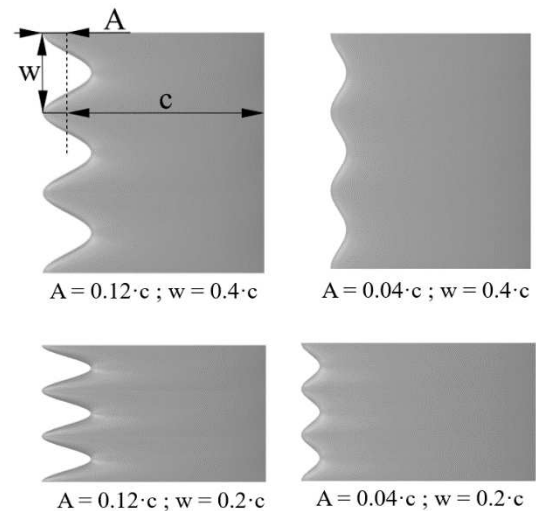


Figure 1. Selected tubercle configurations

Studies by Johari [7] and Hansen et al. [8] demonstrate that with higher amplitudes the flow around the wing is more influenced by the tubercles and therefore lift and drag are changed more compared to a wing without tubercles. This can be seen in the study by Johari [7] where a small amplitude of $A = 0.025 \cdot c$ only reduces maximum lift slightly and improves post-stall lift by a small amount while versions with a high amplitude of $A = 0.12 \cdot c$ have a higher reduction of maximum lift but also higher lift in the post-stall regime.

The influence of the tubercle wavelength does not appear to be as decisive as that of the amplitude. Also, no general rule for the influence of the wavelength can be found in the studies presented here. However, at high wavelengths such as e.g. $w = 0.86 \cdot c$ tested by Hansen et al. [8], the flow behaviour on the wing tends to be very similar to that on the unmodified wing.

2.3. Hypotheses

Even if research findings to date cannot be directly transferred to the application in axial pumps, due to the completely different profile requirements, hypotheses related to the subject of the study can still be derived. These are:

1. The profiles with tubercles do not reach the maximum lift coefficient c_L of the profile without tubercles but show better lift behavior in the post-stall area.
2. The drag coefficient c_D of the profiles with tubercles will be slightly higher for angles without flow separation compared to the reference wing.
3. The lift behavior of the profile with tubercles depends on the configuration used.
 - a. Smaller amplitudes result in higher maximum lift, but only minor improvements in the post-stall area.
 - b. Larger amplitudes result in lower maximum lift, but better post-stall behavior.
4. A smoother stall characteristic can be expected on the tubercled wings than on the baseline wing.

These hypotheses are to be examined in the present study using a CFD simulation.

3. METHOD

As already mentioned, previous research findings cannot be transferred, among other things due to the different profile requirements for axial pumps. Therefore, the profile selection and the selection of the tubercle configurations to be simulated are discussed here first before the setup of the CFD simulation is described.

3.1. Profile Selection and Selected Configurations

The essential profile requirements for axial pumps include slimness combined with a high thickness reserve reducing the suction peak at the leading edge and therefore making the pump vanes less prone to cavitation. Furthermore, a high maximum glide ratio in the design point is desired for a high efficiency of the pump [9]. The chosen Goe11K is shown in Figure 2.

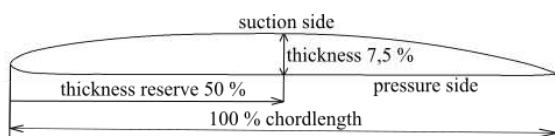


Figure 2. Selected profile Goe11K

This profile meets these requirements [10] and was already used in axial pumps at the Department of Fluid System Dynamics at the Technical

University of Berlin, so previous test results can be compared.

Four configurations of tubercled wings and the baseline version were simulated to investigate a variety of different designs while keeping computational efforts at a reasonable level. A preselection of amplitudes and wavelengths was made considering the analysis made by Hansen et al. [8]. From these studies the configurations were selected to stay within a presumably promising range. Four configurations were created by combining two amplitude values with two values for the wavelength. The selected amplitudes are $A = 0.04 \cdot c$ and $A = 0.12 \cdot c$ and the wavelengths $w = 0.2 \cdot c$ and $w = 0.4 \cdot c$. The leading edge of the baseline wing was taken as the axis around which the defined sinus curve oscillates. This was done to ensure that the projected wing area on the modified wings is the same as on the reference. The four resulting configurations can be seen in Fig. 1. With those wings a wide range of amplitude-to-wavelength-ratios A/w is covered. Reaching from $A/w = 0.1$ for the smoothest up to $A/w = 0.6$ for the sharpest tubercles. Each of the four configurations and the reference profile without tubercles were simulated in the α range from 0° to 24° , with 3° intervals each, with a Reynolds number of $Re = 1.5 \cdot 10^6$.

3.2. CFD Setup

The CFD model was set up with the use of OpenFOAM and according to general information and guidelines on CFD setup e.g. from Schwarze [11]. The presented CFD model reflects an instationary and incompressible flow state and makes use of the RANS-approach. Turbulence in the domain is modelled using the $k\omega$ SST-model as described in [11], a two-equation-model, which reflects turbulence in the freestream and the boundary layer well. Due to the addition of only two new variables, the turbulent kinetic energy k , and the specific dissipation ratio ω , computation time is kept at a reasonable level while still achieving a good depiction of turbulence in the domain. Because of those properties, it is industrial standard and used in this paper.

The calculation domain (cf. Figure 3) was designed to reflect an infinite vane. Therefore, both sidewalls were set to a symmetry condition.

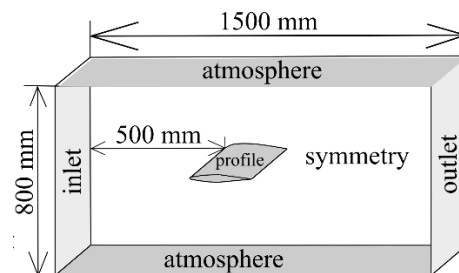


Figure 3. Calculation domain

The created mesh is an unstructured mesh consisting of roughly two million cells. The freestream cells are tetraeders while the boundary layers around the wing are resolved using prism layers. The resolved boundary layers were needed to ensure accurate drag and lift predictions.

Solving was done using the solver `pisoFoam` , which uses the PISO-algorithm. For discretisation of convective terms, the selected scheme was Gauss linear upwind, for the diffusive terms Gauss linear limited 1 was chosen and for gradient terms the Gauss linear scheme was applied. For the temporal discretization the Crank Nicolson scheme was applied with a blending factor of 0.7.

3.3 Mesh study

A mesh study was carried out to ensure that the results are independent from the mesh. To investigate the influence of the mesh resolution on the results, four different resolutions were tested with the baseline wing at $\alpha = 6^\circ$ using the unsteady setup described above. To change the resolution of the mesh, multiple parameters like growth rate of the cells and first layer thickness of the prism layers and thereby y^+ were adapted. For good results the requirement $y^+ < 5$ should be reached in all cells at the wall to keep the cells within the viscous sublayer [11].

Table 1. Overview of the Mesh Study

Cell Count in Million	max y^+	c_D [-]	c_L [-]
0.52	8.809	0.0281	0.998
1.42	7.942	0.0235	1.005
2.195	6.01	0.0194	1.007
4.210	3.74	0.0191	0.993

Table 1 shows the time-averaged force coefficients and the maximum y^+ value for the mesh study. It was found that a poor mesh resolution has a considerable influence on the calculated drag. Between the two highest resolutions the drag value does not vary more than two percent which makes the occurring error tolerable. The maximum y^+ for this resolution is above five. To save computation time the resolution with around two million cells was nonetheless selected for this study, because only around 0.5% of the cells on the wing surface had a y^+ value above five.

The constructed simulation model was validated by comparing the simulated lift and drag behaviour of the Goe11K baseline profile with profile data from Riegels [10]. The results, seen in Figure 4, show good agreement for lift and reasonable agreement for drag.

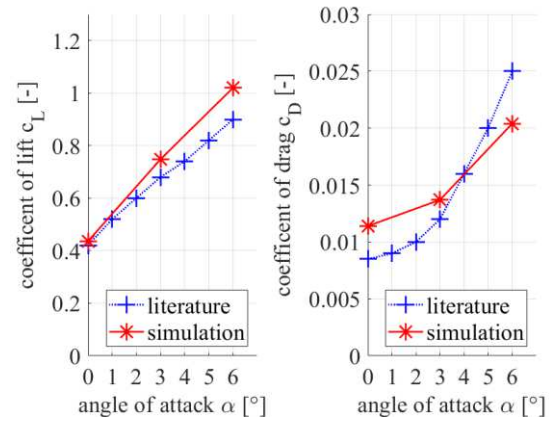


Figure 4. Comparison between simulation results and literature data

4. RESULTS

First, the results of the simulation are presented using the calculated coefficients, after which a qualitative evaluation is carried out using the simulated pressure distribution.

4.1. Quantitative Evaluation

Figure 5 shows the results for the lift coefficients c_L of all tubercle versions and the base wing from the simulation over the simulated α range from 0° to 24° . As can be seen the lift of the baseline wing increases with α up to 18° , where maximum lift of $c_L = 1.6$ is reached. A further increase of α leads to flow separation at the leading edge of the wing. The maximum achievable lift through tubercle configurations is only $c_L = 1.2$. Depending on the tubercle configuration, this corresponds to a maximum loss of lift of about 35%. Furthermore, it was found that all tubercle configurations show a smoother separation behaviour than the baseline.

Apart from that, all tubercle configurations have a higher lift coefficient c_L in the post-stall area than the reference wing. The lift improvement in the post-stall area is the biggest at $\alpha = 21^\circ$ where the tubercles improve lift up to 20%.

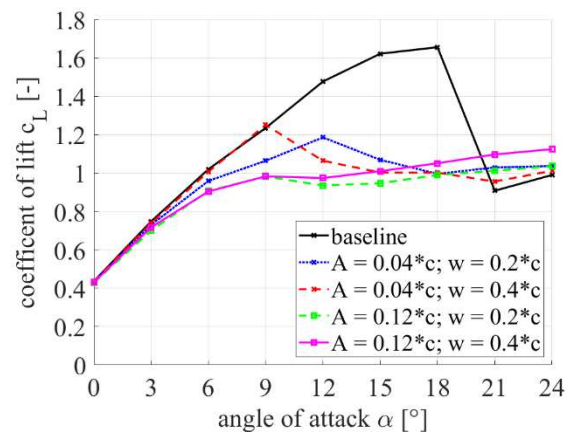


Figure 5. Calculated coefficient of lift c_L for tubercled configurations and baseline

Figure 6 shows the coefficient of drag c_D calculated in the simulations for all versions with modified leading edge and the reference wing plotted over the α range. It is visible that the drag of all configurations between 9° and 18° is higher than on the unmodified wing. In the post-stall-region of the base wing, three of the four tested tubercle configurations achieve lower drag than the unmodified wing.

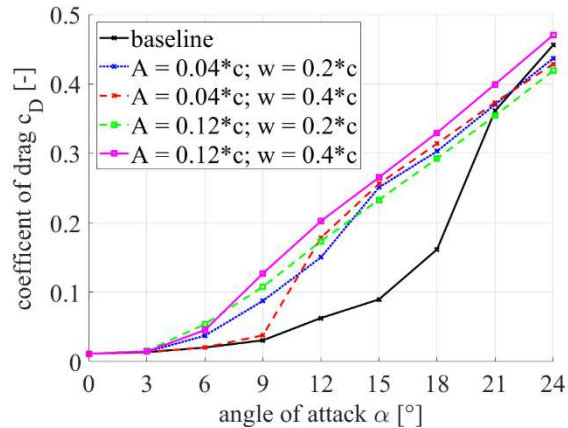


Figure 6. Calculated coefficient of drag for tubercled configurations and baseline

The quantitative evaluation has shown, that the aerodynamical coefficients are heavily influenced by the application of tubercles. The next section is going to determine the reasons for this changed flow behaviour.

4.2. Qualitative Evaluation

In this section the flow around the tubercled wing is analysed using pictures created in post-processing of the simulation. The investigation is started at a low α and is going to describe the changes in the flow field when increasing α to and also beyond the separation angle of the reference wing.

Figure 7 compares the pressure distribution on the suction side of the basewing (the upper wing in Fig. 7) with that of one selected configuration for $\alpha = 3^\circ$. For this comparison the surface is coloured by the local pressure, where blue symbolises low pressures and orange high pressures. The reference wing has a uniform pressure distribution along the whole width while on the tubercled wing a higher negative pressure can be observed in the tubercle valleys than on the tips. The observed negative pressure also exceeds the suction peak of the reference wing.

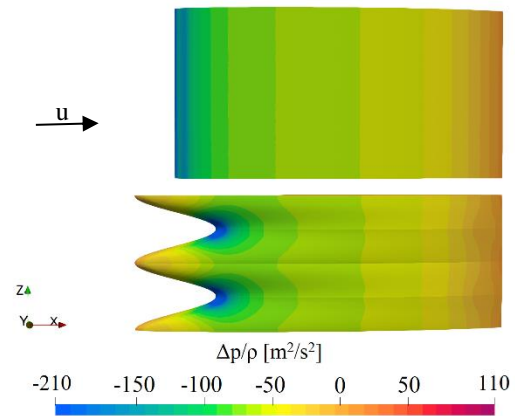


Figure 7. Pressure distribution on the base wing and the tubercle configuration with $A = 0.12 \cdot c$ and $w = 0.2 \cdot c$ at $\alpha = 3^\circ$

When looking at the simulation results it was found that on the simulated wings with the amplitude of $A = 0.12 \cdot c$ a pair of vortices, which can be seen in Figure 8, starts to develop only behind the tubercle valleys on the suction side at $\alpha = 6^\circ$ and above. Fig. 8 shows the surface of the selected tubercle configuration, which is coloured depending on the local pressure. In addition, streamlines are shown in grey to highlight the flow above the wing and to show the vortex behind the tubercle valley. These vortices, although they create some negative pressure and hence vortex lift at the surface, are the reason for the reduction in lift, since the vortex lift is less than the lift present on the wings with fully attached flow, and also the reason for the increase in drag observed in Figures 5 to 6 for these configurations. The vortices mentioned grow when increasing α .

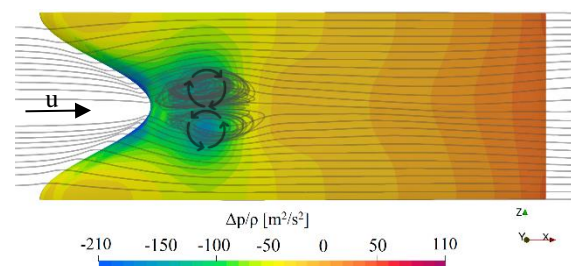


Figure 8. Pair of vortices on the configuration with $A = 0.12 \cdot c$ and $w = 0.2 \cdot c$ at $\alpha = 6^\circ$

Regarding the separation behaviour it was found that some configurations already lose c_L compared to the baseline wing at $\alpha = 6^\circ$ resulting from the mentioned vortices. However, the flow on the configuration with the lowest amplitude-to-wavelength ratio of $A/w = 0.1$, which is the version with the smoothest tubercles, stays completely attached until $\alpha = 9^\circ$. At $\alpha = 12^\circ$ the flow on a major part of this wing is separated, as shown in Figure 9, but a high negative pressure is still present on the tubercle tips.

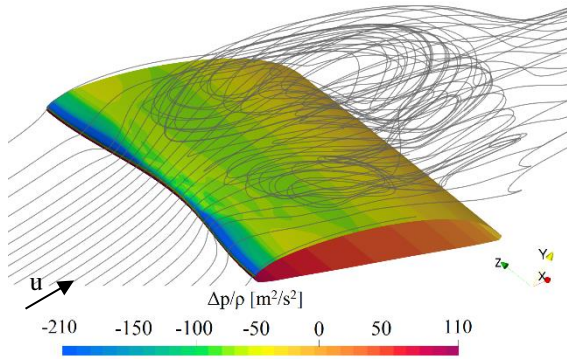


Figure 9. Flow on the configuration with $A = 0.04 \cdot c$ and $w = 0.4 \cdot c$ at $\alpha = 12^\circ$

The flow on the reference wing remains attached up to an $\alpha = 18^\circ$. While increasing α the suction pressure on the leading edge increases to very high values. Regarding these high simulated negative pressures, it should be mentioned, that cavitation could appear at those points when used in water, which strongly influences the behaviour of a pump.

Above $\alpha = 18^\circ$ the wing without tubercles stalls and as a result the achieved lift is rapidly reduced. In comparison the flow on the tubercled wings is still attached at small parts of the wing behind the tubercle tips (cf. Figure 10) at these high α .

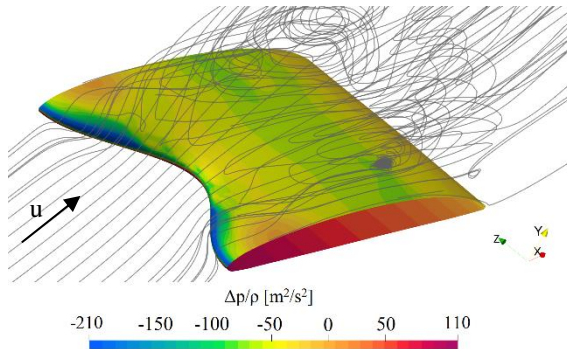


Figure 10. Partly attached flow on the tubercled wing with $A = 0.12 \cdot c$ and $w = 0.2 \cdot c$ at $\alpha = 21^\circ$

5. DISCUSSION

The simulation results show that for the selected profile, setup and Reynolds number improvements in post-stall lift can be found, while there is a loss at lower α . Therefore, the first hypothesis is confirmed. However, the magnitude of this trend has been underestimated and appears large compared to the literature e.g. [6]. The loss in lift in the pre-stall region of around 35% is large while the improvement in post-stall is smaller with around 10% to 20%. The best tested configuration is the one with the amplitude of $A/c = 0.12$ and the wavelength of $w/c = 0.4$. While the loss of this version at low angles is comparable to the version with the same tubercle amplitude, the lift is the highest for all tubercle configuration from $\alpha = 18^\circ$ upwards.

Regarding the second hypothesis, which stated that drag values in the area of adjacent flow should be slightly higher for the tubercled versions, it can be argued that again the overall trend follows this hypothesis but the extent to which the drag is increased is, with around 50% increase compared to the baseline, greater than expected. Therefore, the hypothesis can not be verified because only a minor increase in drag was expected, but the results showed a rather significant increase.

The differing results compared to the literature can be attributed to multiple factors.

Firstly, the chosen Goe11K profile is with a thickness of 7.5% chord slimmer than profiles described in literature. It is designed to achieve a high glide ratio at low α . This leads to a significant increase in drag when vortices start to appear behind the tubercle valleys at $\alpha = 6^\circ$, where the drag of two tubercled configurations is more than doubled (cf. Fig. 6). Secondly the approach of an infinite wing does not show the benefit of tubercles created through spanwise flow suppression, which can be seen when comparing results from Miklosovic et.al. [3] and Cai et.al. [6]. When using the infinite wing model, the third working mechanism of tubercles (see chapter 2.) does not improve flow around the wing, because no spanwise flow appears due to the absence of a spanwise pressure gradient or spanwise forces, that could be suppressed. However, the infinite wing approach more closely reflects the conditions in an axial flow pump than a finite wing because the casing suppresses the formation of tip vortices. Thirdly, a study by Dropkin et al. [12] has shown that the maximum lift on a tubercled wing does not increase in the same way the maximum lift of an unmodified wing does at higher Reynolds numbers. Therefore, the selected Reynolds number of $Re = 1.5 \cdot 10^6$, which is high compared to most studies on tubercle application, results in a larger difference in maximum lift between base wing and tubercle configurations. Lastly, it must be noted that the lift on the base wing at high α from 12° to 18° can partly be attributed to the simulated high negative pressures. When using tubercles in an axial pump with water as the pumping medium those high negative pressures could lead to cavitation on the leading edge and therefore lift would be reduced. As a result, the difference in lift between tubercle configurations and baseline wing at those α might be smaller in reality.

The third hypothesis, which claimed that the lift behaviour depends on the selected tubercle configuration, is confirmed when looking at the simulation results. The versions with a smaller amplitude follow the lift slope of the unmodified wing up to $\alpha = 9^\circ$ and achieve a higher maximum lift in the pre-stall area of the baseline than the version with higher amplitude. Furthermore, on these configurations a sudden decrease in lift can be found at $\alpha = 9^\circ$ or $\alpha = 12^\circ$. This is due to the fact, that at

those α a vast area of the wing stalls, decreasing lift. This effect cannot be observed on the tubercle configurations with the higher amplitude. The lift does not increase as much as on the other versions at low α but also does not drop noticeably at any α . This is due to the smoother separation behaviour on those wings. In the post-stall region only the version with the wavelength of $w/c = 0.4$ has a better lift value than the configurations with the lower amplitude. This might be due to the fact, that the amplitude-to-wavelength ratio on the configuration with $A/c = 0.12$ and $w/c = 0.2$ might be too high.

The fourth hypothesis, dealing with the stall characteristic, can also be accepted. The separation behaviour on the tubercled versions is indeed smoother than on the baseline wing. While no tubercled versions shows a rapid lift decrease like the baseline does, the lift on the versions with the small amplitude of $A/c = 0.04 \cdot c$ does drop slightly at $\alpha = 9^\circ$ resp. $\alpha = 12^\circ$. In contrast the lift curve for the wings with the higher tubercle amplitude do not show a drop in lift at any α .

6. CONCLUSION

From the simulation results and from the studies presented in chapter 2 it can be concluded that the benefit of tubercles comes in operation points where a flow separation on unmodified wings/blades is likely. For axial pumps this is the case in operation points well below the design point. In the simulation it was shown that an optimized tubercle configuration can improve lift at those points by 20%, while maintaining similar drag values. This is because tubercles not only delay flow separation by energizing the boundary layer at the trailing edge, but also confine appearing separation zones locally. As a result, on larger parts of the blades the flow should stay attached for longer.

In addition, the application of tubercles would also most likely reduce or completely erase the phenomenon called “rotation stall” described in [9], where a stalled region rotates in opposite direction to the blades. This is because of the smoother separation characteristics of the tubercled blades compared to the version with conventional leading edge.

Concerning Reynolds number, it can be concluded, that the selected Reynolds number of $Re = 1.5 \cdot 10^6$, which was chosen based on an existing pump with an outer diameter of $d_A = 149 \text{ mm}$, an average chord length of around $c = 100 \text{ mm}$ and a rotational speed of $n = 2865 \text{ rpm}$ in the design point, reduces the positive effect of the tubercles. The use of tubercles in axial pumps with a lower Reynolds number, due to a smaller chord length of the blades or a lower rotational speed, could be more advantageous.

In the design point, which would be at around $\alpha = 3^\circ$, where the highest glide ratio is achieved on the reference wing, lift and drag on the tubercle

configurations are not changed by much, the maximum glide ratio is reduced from 54 to around 50 depending on the selected configuration. However, when increasing α the efficiency and lift of the unmodified wing cannot be achieved with tubercles. Compared to studies shown in chapter 2 the difference between unmodified and tubercled wings is bigger in the presented simulation. Reasons for that were described to be the profile selection, Reynolds number and the model of the infinite wing. Regarding profile selection, tubercles seem to be less effective on profiles needed for axial flow pumps than on thicker profiles used for other applications. In the matter of the selected infinite wing model, it is true that axial pump blades do not show a free tip like on e.g. airplane wings, where spanwise flow is to be expected, because of the casing around the blades. However, crossflow can nonetheless be expected to a certain extend because of centrifugal forces or partial flow separation on the blades.

Another important influence on axial pumps is cavitation. It was already briefly mentioned in the discussion, that the appearance of cavitation might change results. However, the simulation was not set up to cover this phenomenon and therefore the influence of cavitation could not be investigated on. Research by Johari [7] suggests that tubercles influence cavitation behaviour depending on the selected configuration. In this study [7] a wing with a NACA 63₄-021 was tested with different tubercle configurations at $Re = 7.2 \cdot 10^5$ and a range of α from 12° to 24° . For versions with low amplitudes and higher wavelengths the cavitation characteristics is similar to that of the baseline wing. On the whole leading edge of the wing sheet cavitation appears and increases in size with higher α . On configurations with higher amplitudes and smaller wavelength cavitation appears earlier than on the baseline wing but is confined to the regions behind the tubercle valleys for all α . Sheet cavitation did not appear on those wings. Because only the area behind the tubercle valleys is affected by cavitation on these wings, lift can still be created on the tubercle tips. Since the simulation has shown that a major part of the lift is created in the affected region it remains unclear whether the total lift created by these configurations under cavitation conditions really is higher than on an unmodified wing.

Nonetheless, it is likely that the evenly lift behaviour due to the smoother separation of the wings with tubercles enlarges a pump's operating range, with benefits in the application.

Overall, tubercles on axial pumps are expected to bring overall improvement, if a wide operation range, good efficiency and suction head are required, especially at low speed well below the operation point.

7. SUMMARY AND OUTLOOK

Due to missing research on the application of tubercles in axial pumps the aim of this study was to determine possible influences of tubercles when used on axial pump vanes. The Goe11K profile was selected for the simulation because it is a slim profile with a high thickness reserve and consequently well suited for the use in axial pumps.

The Reynolds number was chosen to be $Re = 1.5 \cdot 10^6$ based on an existing axial pump tested previously. Four tubercled wings were selected based on the results of earlier studies [7, 8] covering a good spectrum of amplitudes and wavelengths. The simulation was set up as a transient and incompressible CFD-simulation in OpenFOAM. using the model approach of an infinite wing. This set up was selected to keep computational effort at a reasonable level making it possible to investigate four tubercle configurations at a large α range. A mesh independence study was carried out to make sure results are not reliant on the discretisation of the domain. The simulation results show only small improvements in the post-stall area due to the leading-edge tubercles, while a significant reduction in maximum lift in the pre-stall area was observed. This was attributed to the selected Reynolds number, profile selection and infinite wing model. In the discussion an aspect outside the simulation model "rotation stall" was considered as well. Leading to the conclusion that the benefit of tubercles at lower Reynolds numbers might be higher than in the simulation. Furthermore, the simulation results showed that the tubercled wings have a smoother separation behaviour. This gain leading to a wider operation range still comes at a cost of lower lift and higher drag in the design point.

Despite that, it was argued that tubercles could improve axial pumps used at lower Reynolds numbers when a fitting tubercle configuration is selected and a good suction head is needed at low speeds, well below the design point.

Further studies should investigate whether these results can be transferred to applications in axial pumps as expected or whether other effects that have not yet been considered, such as centrifugal forces, dominate the flow. For this purpose, a test bench according to DIN EN ISO 9906 is currently being set up at the Department of Fluid System Dynamics at the Technical University of Berlin. This will be used to investigate the extent to which tubercles on the front edge of the blades of an axial three-bladed pump impeller with the Goe11K profile used in the simulation change the efficiency, the head, the power consumption, and the cavitation behaviour.

REFERENCES

[1] Fish, F. E., and Battle, J. M., 1995, „Hydrodynamic design of the humpback whale flipper”, *Journal of morphology*, Vol. 225 (1), pp. 51-60.

- [2] van Nierop, E. A., Alben, S., and Brenner, M. P., 2008, “How bumps on whale flippers delay stall: an aerodynamic model”, *Physical review letters*, Vol. 100 (5), p. 54502
- [3] Miklosovic, D. S., Murray, M. M., Howle, L. E., and Fish, F. E., 2004, “Leading-edge tubercles delay stall on humpback whale (Megaptera novaeangliae) flippers.”, *Physics of Fluids*, Vol. 16 (5), pp. L39-L42.
- [4] Pedro, C., and Kobayashi, M., 2008, “Numerical Study of Stall Delay on Humpback Whale Flippers.”, *46th AIAA Aerospace Sciences Meeting and Exhibit*, Reno, Nevada
- [5] Custodio, D., 2007, “The Effect of Humpback Whale-like Protuberances on Hydrofoil Performance.” *Master thesis, Worcester Polytechnic Institute.*
- [6] Cai, C., Zuo, Z. G., Liu, S. H., Wu, Y. L., and Wang, F. B., 2013, “Numerical evaluations of the effect of leading-edge protuberances on the static and dynamic stall characteristics of an airfoil.”, *IOP Conf. Ser.: Mater. Sci. Eng.*, Vol. 52 (5), p. 52006.
- [7] Johari, H., 2007, “Effects of Leading-Edge Protuberances on Airfoil Performance”, *AIAA Journal*, Vol. 45 (11), pp. 2634-2642
- [8] Hansen, K. L., Kelso, R. M., and Dally, B. B., 2011, “Performance Variations of Leading-Edge Tubercles for Distinct Airfoil Profiles.”, *AIAA Journal*, Vol. 49 (1), pp. 185-194.
- [9] Pfleiderer, C., and Petermann, H., 2005, *Strömungsmaschinen*, 7. Edition, Berlin, Springer.
- [10] Riegels, F. W., 1961, *Aerofoil Selections. Results From Wind-Tunnel Investigations*, London, Butterworth & Co
- [11] Schwarze, R., 2013, *CFD-Modellierung*, Berlin, Springer
- [12] Dropkin, A., Custodio, D., Henoch, C. W., and Johari, H., 2012, “Computation of Flow Field Around an Airfoil with Leading-Edge Protuberances”, *Journal of Aircraft*, Vol. 49 (5), pp. 1345-1355